PROTEINS: Structure, Function, and Genetics 34:173–183 (1999)

Modelling of Factor Xa-Inhibitor Complexes: A Computational Flexible Docking Approach

Mohan S. Rao and Arthur J. Olson*
Department of Molecular Biology, The Scripps Research Institute, La Jolla, California

ABSTRACT **In order to understand the structural basis of Factor Xa (FXa) specificity, structural complexes of FXa with its synthetic inhibitors are determined using a computational docking approach. The AutoDock suite of programs is used to determine the binding modes of the synthetic inhibitors such as 3- and 4-amidinobenzylphenyl ether (ABP), amidinophenyl pyruvic acid (APPA), diamidinobenzofuranyl ethene (DABE), and DX-9065a 2-(5′-amidino-2′-benzofuranyl)-3-(7′amidino-2′-napthyl)-propionic acid (ABAP) to FXa. The synthetic inhibitors docked in the present study are different in size, nature of linkage, and properties. Two sets of simulations were carried out for synthetic inhibitors docking to FXa. In the first set of simulations, no explicit water molecules were included. In the second set of simulations two explicit solvent molecules were considered. In all the computationally predicted synthetic inhibitor complexes of FXa, the specificity pocket residue Asp-189 is involved in hydrogen bonding with the bound inhibitor. The active site water molecule WAT522 is involved in hydrogen bonding with all the bound inhibitors. The computed energies clearly discriminate the high affinity from low affinity binders. Proteins 1999;34:173–183.** © 1999 Wiley-Liss, Inc.

Key words: protein-ligand interaction; flexible docking; blood coagulation; serine protease; synthetic inhibitors; Factor Xa

INTRODUCTION

Factor Xa (FXa) is a serine protease involved in the blood coagulation cascade.[1–3] Under physiological conditions FXa catalyses the conversion of prothrombin to thrombin.[4,5] Both the extrinsic and intrinsic pathways of the coagulation cascade converge at the stage of FXa. Therefore inhibition of FXa may provide effective interference to the blood coagulation process. FXa can be inhibited by simple inhibitors such as 3- and 4-amidinobenzylphenyl ether (ABP),[6] diamidinobenzofuranylethene (DABE), [7] DX-9065a,[8] 2-(5′-amidino-2′-benzofuranyl)-3-(7′-amidino-2′-naphthyl)-propanoic acid (ABAP)[9] as well as by macromolecular inhibitors such as Tick Anticoagulant Peptide (TAP).[10,11]

Factor Xa consists of four domains with marked sequence and structural homology to other coagulation enzymes. The gamma carboxyl glutamic acid (Gla)-rich domain consists of 40 amino acids at the amino terminus. The Gla residues are critical for calcium dependent interaction between FXa and phospholipid. This is followed by two epidermal growth factor domains (EGF), each approximately 40 amino acids in length. They each contain six cystine residues and form three intra-chain disulfide bonds, a characteristic of EGF modules. A serine protease domain is attached to the second EGF domain by an inter-chain disulfide bond.

The three dimensional structure of FXa has been reported at 2.2 Å.[12] The reported structure describes two domains, namely the protease domain and the second EGF domain. These two are connected by a disulfide bridge. The catalytic domain of FXa exhibits a high degree of homology with trypsin-like serine proteases. In the reported crystal structure of the trypsin-benzamidine complex, two amidine hydrogens of the benzamidine are hydrogen bonded to the side chain oxygen of Asp-189.[13] The structures of thrombin-benzamidine derivative complexes suggest the involvement of this specificity pocket residue, Asp-189, in inhibitor/substrate recognition for this class of proteins.[14]

Rezaie and Esmon[15] have observed, based on site-directed mutagenesis experiments, that the Gln-192-Glu mutation in a Gla-less FXa diminishes the inhibitory effect by 30 fold of the Kunitz-type inhibitors. It is known that the other blood coagulation enzymes such as thrombin and protein C have Glu at the 192 position. These enzymes (Glu at 192 position) are resistant to inhibition by Kunitz inhibitors, but FXa with Gln at this position is effectively inhibited by Kunitz inhibitors.

The 3- and 4-amidinobenzylphenyl ethers and ketones are simple inhibitors of FXa.[16] Binding studies suggest that 3-amidino derivatives are stronger inhibitors than 4-amidino derivatives. Substitution of a methyl group for an amidine group in any of the above derivatives abolishes the binding. On the other hand similar substitution at the 3- or 4- position of the benzyl ring does not affect the binding. Substitution of an acidic group at the 3- or 4- position of the benzene ring alters the binding activity.

Dibasic propanoic acid derivatives are shown to inhibit the FXa at low concentrations.[7] These inhibitors are better binders than the amidinobenzylphenyl ethers. A new synthetic inhibitor, DX-9065a, is shown to inhibit the FXa

Grant sponsor: National Institutes of Health; Grant number: PO1 HL16411.
*Correspondence to: Arthur J. Olson, Department of Molecular Biology, The Scripps Research Institute, 10550 N. Torrey Pines Road, La Jolla, CA 92037. E-mail: olson@scripps.edu
Received 14 April 1998; Accepted 5 October 1998

at nanomolar concentrations.[17] Katakura et al.[18] have synthesized DX-9065a and have studied structure/activity relationships by constructing models of FXa complexed with this synthetic inhibitor based upon X-ray crystallographic data from a trypsin-inhibitor complex. In the constructed model, the benzamidine group of the inhibitor is placed in the specificity pocket. Lin and Johnson[19] have constructed a model of FXa complexed with DX-9065a based on the X-ray structure of the thrombin-benzamidine complex. In the generated complex, the amidine group of the inhibitor was placed in the specificity pocket. Stubb et al.[20] have solved the crystal structures of FXa inhibitors bound to the beta trypsin. Based on these structures, they constructed a model of FXa-DX-9065a complex. In this model also the amidine group was placed well into the specificity pocket. However, none of these models were built using explicit solvent molecules.

Thus, the above studies provide valuable information, suggesting some features of the binding of inhibitors to FXa. These include the involvement of Asp-189 and Gln-192 residues in binding synthetic inhibitors; involvement of the amidine group of the bound ligand; and the relative inhibitory potency of various inhibitors. However, little or no information is available on the possible binding modes of these inhibitors to FXa. Hence, in the present study an attempt has been made to determine the most probable binding modes and interactions of these inhibitors to FXa both in the presence and absence of explicit solvent molecules using our computational docking approach. These studies help not only in understanding the modes of binding of the inhibitors to FXa but also provide a stereochemical explanation for their experimentally-observed binding affinities.

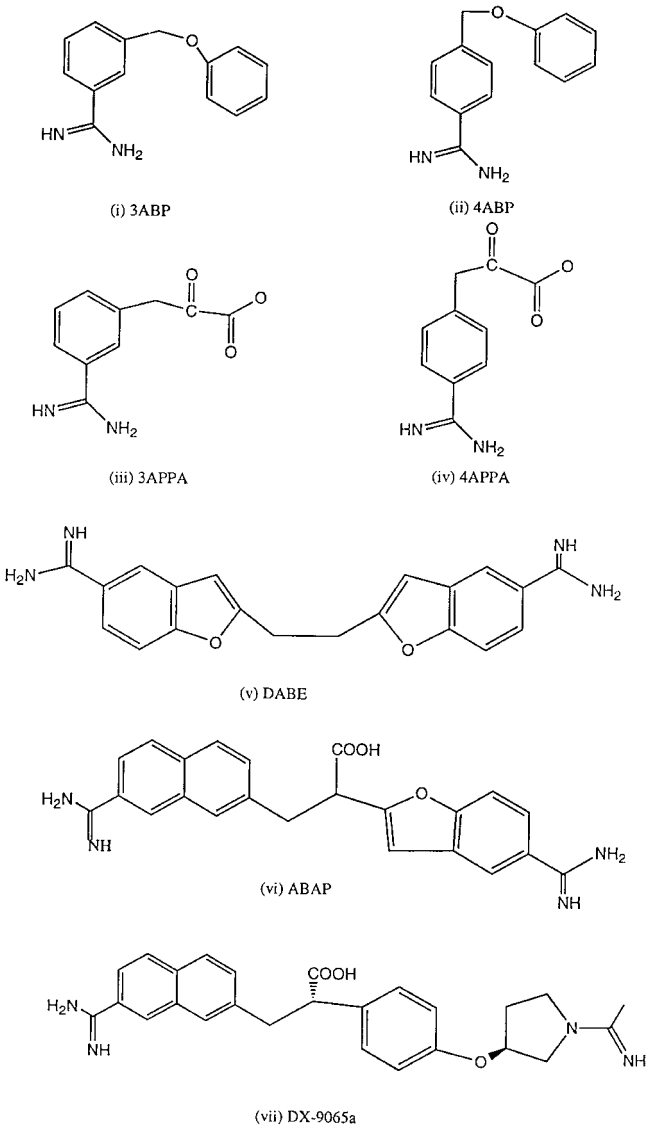

Fig. 1. Schematic diagram of synthetic inhibitors of FXa.

COMPUTATIONAL PROCEDURES

Flexible Inhibitor Docking

AutoDock, an automated docking approach described in full elsewhere,[21, 22] starts a ligand molecule in an arbitrary conformation, orientation, and position and finds favorable docked configurations in a protein binding site. Simulated annealing is used to explore the conformational space. In this approach, the ligand performs a random walk around the static protein. At each time step, the ligand is moved by a small increment in global translation and orientation and in each of the rotatable torsion angles. The new configuration is accepted or rejected based upon a temperature-dependent probability expression. A typical simulation is started at high temperature allowing the acceptance of high-energy interactions in order to escape local minima. As the simulation proceeds, the temperature is reduced, slowly constraining the ligand to occupy only favorable regions. At each step of the simulation, the energy of interaction of ligand and protein is evaluated using atomic affinity potentials computed on a grid similar to that described by Goodford.[23] In a pre-calculation the protein is embedded in a three-dimensional grid and a probe atom is sequentially placed at each grid point. The energy of interaction of this single atom with the protein is assigned to the grid point. An affinity grid is calculated for each type of atom in a ligand as well as for the electrostatic interactions.

Interaction energies are calculated with a free-energy-based expression comprising terms for dispersion/repulsion energy, directional hydrogen bonding and screened Coulomb potential electrostatics, as well as a volume-based solvation term similar to that of Stouten et al.[24] and a simple weighted sum of torsional degrees of freedom to estimate the entropic cost of binding, similar to that used by Bohm.[25] The force field was calibrated with thirty chemically diverse protein:ligand complexes, and successfully predicted the experimental binding energies of twenty HIV-1 protease-inhibitor complexes with a 1.8 kcal/mol RMS deviation.[26]

To model FXa-synthetic inhibitor complexes, the coordinates of FXa at 2.2-Å resolution were taken from the Protein Data Bank (1hcg). Initially we did not consider any

TABLE I. Docking Results of FXa-Inhibitor Complexes

		Explicit solvent		Without solvent		Experimental
Inhibitor	Rank	Number in each cluster	Computed free energy Kcal/mol	Number in each cluster	Computed free energy Kcal/mol	binding energy Kcal/mol
4ABP	1	6	−8.57	4	−8.73	−4.66
	2	3	−8.56	3	−8.31	
	3	3	−8.32	1	−8.28	
	4	3	−8.21	5	−8.22	
	5	6	−7.92	5	−7.84	
3APPA	1	2	−8.15	4	−6.20	−4.98
	2	3	−8.05	1	−6.00	
	3	3	−7.43	1	−5.82	
	4	1	−7.17	4	−5.80	
	5	1	−7.16	1	−5.70	
3ABP	1	2	−8.90	1	−8.82	−7.02
	2	4	−8.86	5	−8.54	
	3	4	−8.85	1	−8.35	
	4	1	−8.80	1	−8.30	
	5	1	−8.69	1	−8.23	
DABE	1	4	−12.39	5	−13.69	−8.62
	2	6	−12.01	1	−12.59	
	3	2	−11.58	1	−12.53	
	4	1	−11.40	2	−12.49	
	5	1	−11.34	2	−12.48	
ABAP	1	4	−11.29	3	−11.88	−10.96
	2	2	−10.68	2	−11.43	
	3	1	−10.45	1	−10.48	
	4	1	−10.21	1	−10.40	
	5	2	−10.14	2	−9.92	
DX-9065a	1	3	−11.11	2	−10.69	−10.14
	2	2	−10.95	1	−10.33	
	3	4	−10.52	1	−10.22	
	4	1	−10.12	2	−9.87	
	5	1	−9.77	3	−9.54	

explicit water molecules in our calculations. However, in another set of simulations two active site water molecules (WAT 514 and WAT 522) were considered explicitly to study the effect of these water molecules in inhibitor binding. No protein atoms were allowed to move during the simulation. Hydrogen atoms were fixed to polar atoms using the SYBYL molecular modeling package (Tripos Associates, Inc., St. Louis, MO). The CH, CH_2, CH_3 groups of the amino acid residues were treated as united atoms by adjusting van der Waals parameters and partial atomic charges suitably. Grids were calculated with 80 elements on side ($80 \times 80 \times 80$) and spacing of 0.4 Å centered on the Cβ of the catalytic residue His 57. During the simulated annealing experiment, the torsional angle defining the orientation of the amidine group in each of the inhibitor was fixed in the plane of the benzene ring owing to the delocalization of the π-electron cloud. All other rotatable torsions were allowed to vary. The geometries of the inhibitors were generated using the InsightII molecular modeling program (from MSI, San Diego, CA). For each inhibitor the simulation was composed of 100 docking runs, each of 50 cycles containing a maximum of 20,000 accepted or 20,000 rejected steps each, whichever limit was reached first. An input parameter was set to ensure

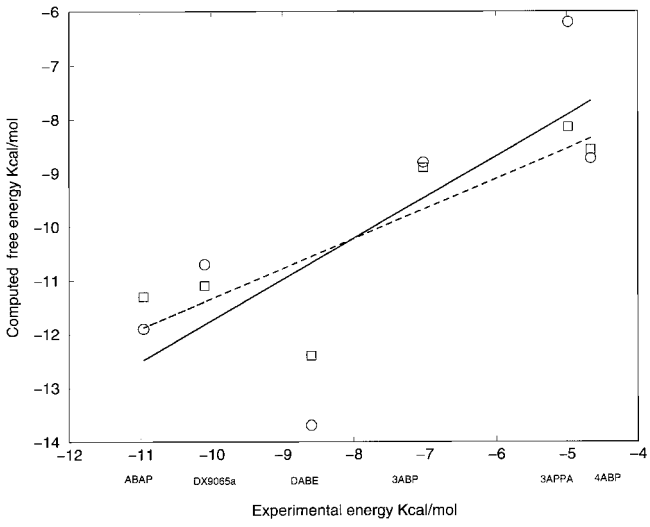

Fig. 2. Plot showing the correlation between computed and experimental binding energies of FXa-inhibitor complexes. The squares and circles correspond to the computed free energies with and without solvent, respectively. The solid and dotted lines correspond to the computed correlations with the experimental binding energies for the models with and without solvent respectively.

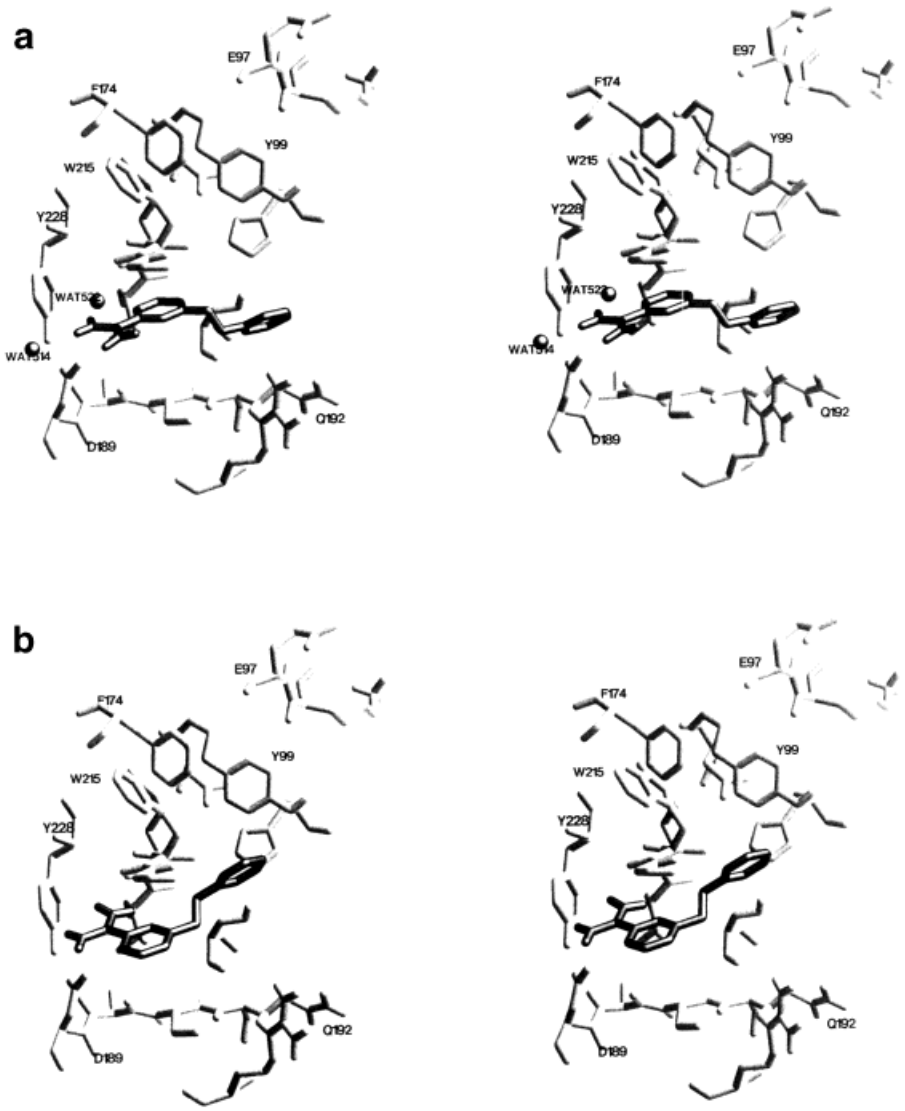

Fig. 3. Mode of binding of 3ABP to FXa: **(a)** with solvent and **(b)** without solvent.

that no runs began with a positive energy. The docked complexes were clustered with an RMSD tolerance of 0.8 Å. Symmetry checking, which, for example, treats the three symmetry-related rotations of a tert-butyl groups as equivalent, is optional in the RMSD calculation. When clustering the complexes, we have not used the symmetry checking in the RMSD calculations presented here, since the united atom approximation eliminated the need to do so. We started these simulated annealing experiments at high temperature (RT = 616 kcal/mol) and decreased it by a factor 0.92 on each cycle. Computational time for 100 dockings on a DEC Alpha 250 workstation was 82 minutes for the largest inhibitor (DX-9065a).

RESULTS AND DISCUSSION

A schematic diagram of all the synthetic inhibitors are shown in Figure 1. These inhibitors, except 4APPA, were docked with FXa using our AutoDock procedure. Since 4APPA binds to FXa covalently we have not considered these complexes. All the computationally predicted lowest energy complexes of FXa are stabilized by intermolecular hydrogen bonds and stacking interactions. In these computed complexes of FXa, the specificity pocket residue Asp-189 of FXa is involved in hydrogen bonding with the bound inhibitor.[27] In the complexes of 3ABP, 4ABP, DABE, ABAP, and DX-9065a, two hydrogen bonds are possible between the amidine hydrogens of the bound inhibitor and the specificity pocket residues Asp-189 and Tyr-228. In the presence of active site water molecules an interaction between the Tyr-228 and the amidine group of the bound inhibitors is not possible. However, in all the predicted complexes a hydrogen bond is possible between the bound inhibitor and the conserved water molecule (WAT522). The interactions in these complexes vary depending on the

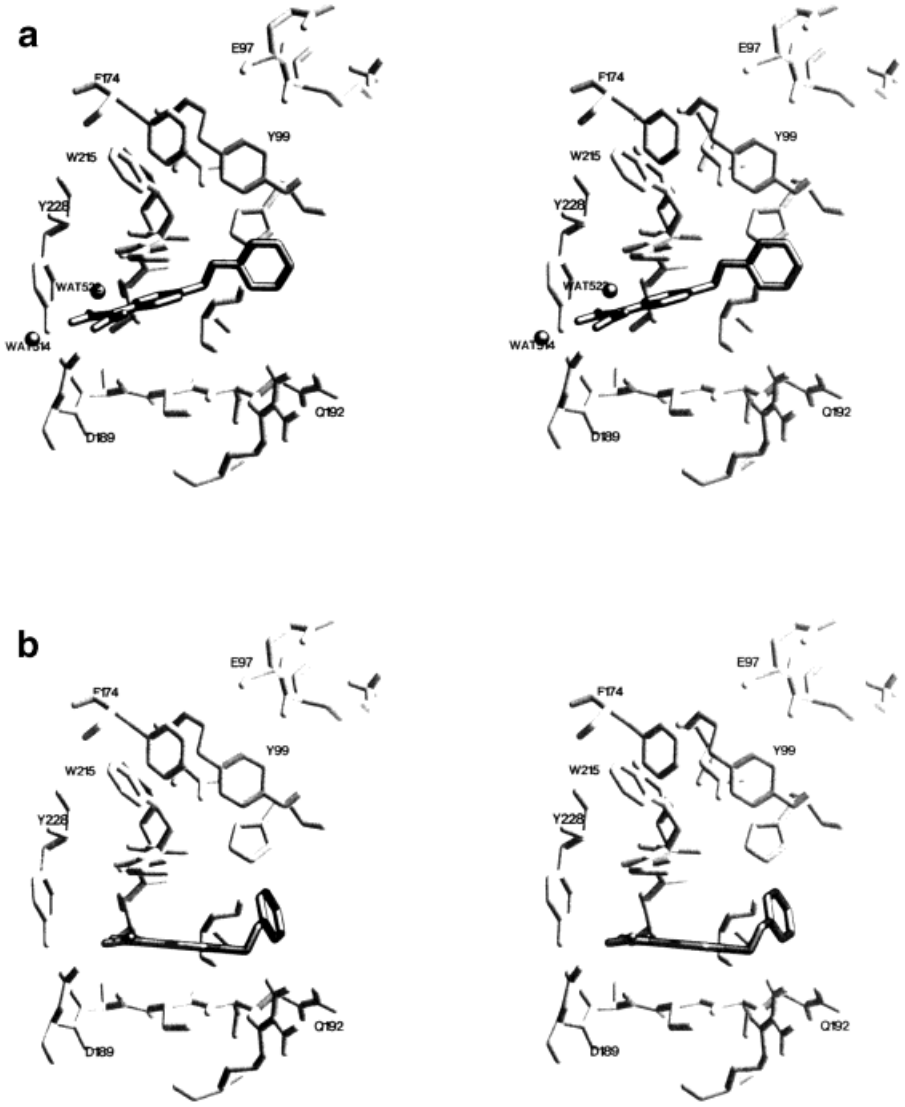

Fig. 4. Mode of binding of 4ABP to FXa: **(a)** with solvent and **(b)** without solvent.

size, linkage, and the functional group. In the case of DABE, ABAP, and DX-9065a complexes, the hydrophobic box region of FXa composed of Tyr-99, Phe-174, and Trp-215 favors a stacking interaction with bound ligands. These stacking interactions have been proposed as the reason for the increased binding affinities of these larger inhibitors.[19]

Table I shows the computed free energies of binding for the top five ranking inhibitor complexes both for the dockings run without and with the explicit water molecules (WAT522 and WAT514). From this Table it is clear that the predicted binding energies of DX-9065a, ABAP, and 3ABP are in agreement with experimental studies. The predicted energies for 4ABP, DABE, and 3APPA are lower than the experimental energies. However, this study clearly discriminates between the higher affinity binders such as DABE, ABAP, and DX9065a from the low affinity binding molecules ABP and APPA. Figure 2 shows a correlation plot between the experimental and computed binding energies. The correlation coefficient is better when the explicit solvent is used in the docking (corr. coef. = 0.83) than when the docking is done without these two waters (corr. coef. = 0.75).

Binding Modes of Synthetic Inhibitors to FXa: Inhibitor-Protein Docking

The most energetically favorable binding mode of 3-amidinobenzylphenyl ether (3ABP) to FXa is shown in the stereo diagram (Fig. 3a). From this figure it can be seen that the benzamidine portion of the 3ABP binds into the specificity pocket. In this pocket the amidine group of 3ABP interacts with the side chain of Asp-189 and an active site water molecule WAT522. In the absence of this water molecule, a direct interaction is possible between the bound ligand and Tyr-228 (Fig. 3b). The energetically favorable mode of binding of 4-amidinobenzylphenyl ether

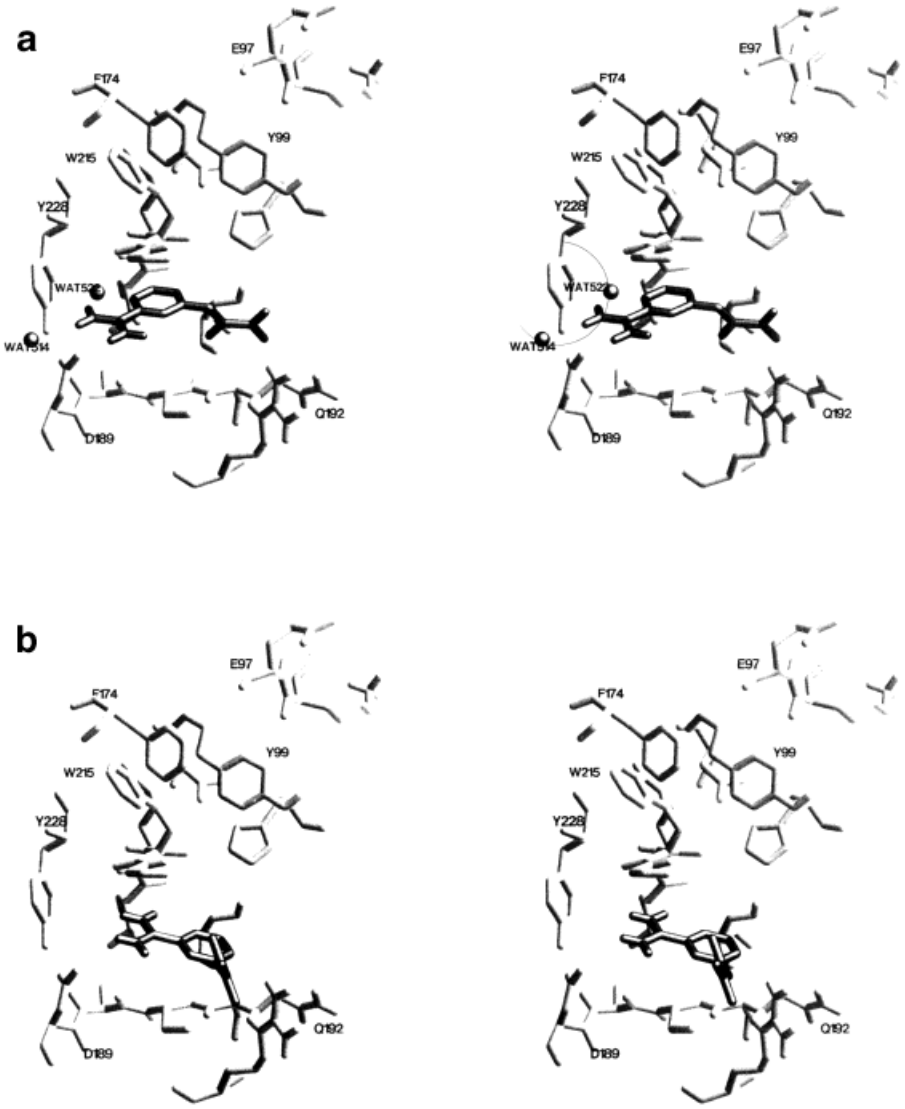

Fig. 5. Mode of binding of 3APPA to FXa: **(a)** with solvent and **(b)** without solvent.

(4ABP) to FXa both in the presence and absence of an active site water molecule are shown in Figure 4a and 4b. In these complexes the benzamidine portion of 4ABP assumes similar orientation of 3ABP at the specificity pocket of FXa. At the specificity pocket, the amidine hydrogens of 4ABP form two hydrogen bonds with the side chain of the Asp-189 and WAT522. In the lowest energy complexes of 3ABP and 4ABP with FXa, the phenyl ring of the bound inhibitors are placed in different locations. The differential placement of the phenyl ring in the 4ABP and 3ABP complexes may explain their differential binding activities. These results suggest that the addition of a functional group at the 3- or 4- position of the inhibitors does not alter the preferred orientation of the benzamidine group at the specificity pocket. The amidinophenyl pyruvic acids (APPAs) differ from the ABPs in the 3-or 4- position substituent. In the latter, the substituent is a phenyl group and in the former it is an acidic group. In the 3APPA complex the amidine group binds at the specificity pocket. The acidic group is placed near the catalytic triad. Figure 5a and 5b shows the binding of 3APPA to FXa both in absence and presence of an active site water molecule.

Di-5-amino-2-benzofuranyl ethene (DABE) is a symmetric molecule. Figure 6a shows the lowest energy complex of FXa-DABE. In this complex, a part of the DABE binds into the specificity pocket and the other end interacts with the hydrophobic region where Trp-215, Tyr-99, and Phe-174 are arranged like a box. Three strong hydrogen bonds are possible between the amidine hydrogens of DABE and the specificity pocket residues Asp-189 and WAT522 of FXa. As can be seen in Figure 6a, the part of DABE within the hydrophobic box has many favorable hydrophobic contacts including ring stacking. These stacking interactions at the hydrophobic region of FXa are perhaps the reason for the higher binding affinity of DABE as well as the other large inhibitors (see below) over ABP and APPA. Figure 6b

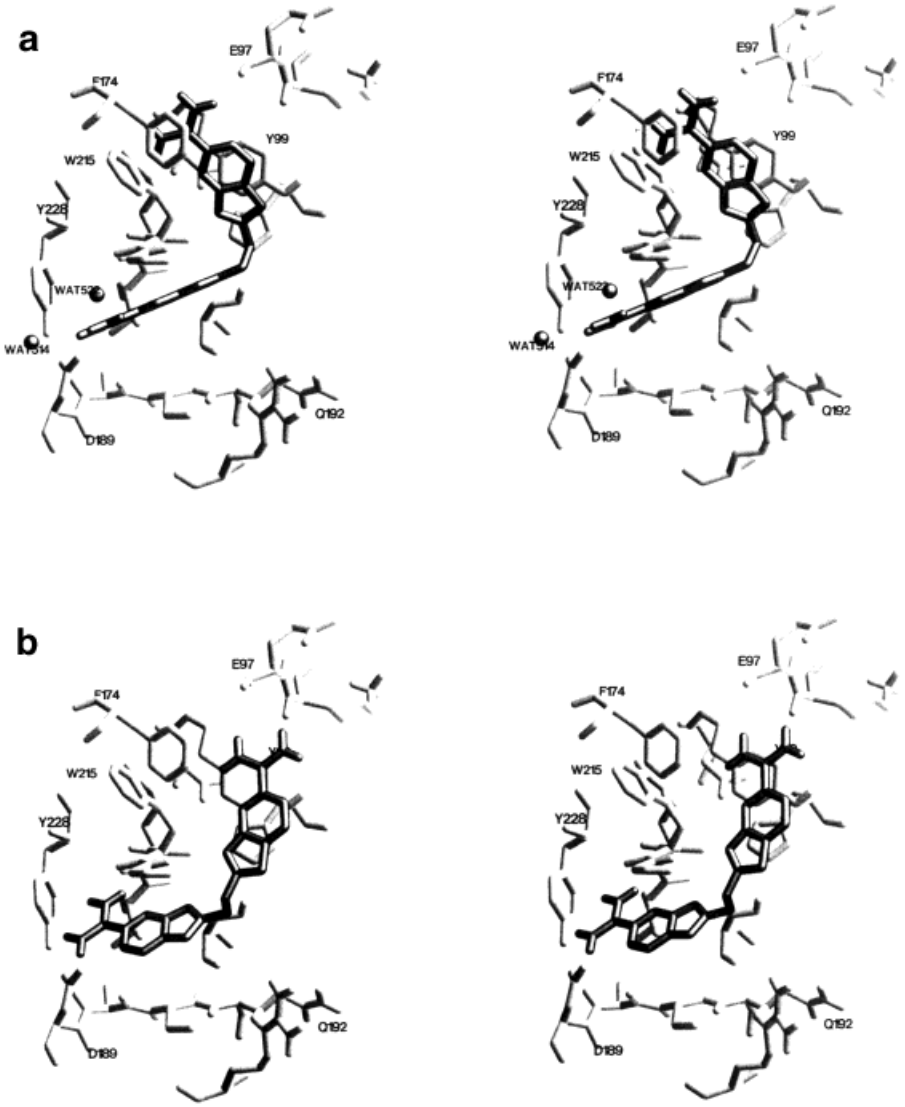

Fig. 6. Mode of binding of DABE to FXa: **(a)** with solvent and **(b)** without solvent.

shows the predicted binding mode of DABE in the absence of explicit solvent molecules. In this binding mode the amidine group at the specificity pocket interacts directly with Tyr-228. It can be seen from Figure 6a that in the presence of WAT522, the amidine group does not bind to FXa as in Figure 6b and in the hydrophobic region of FXa, DABE also favors a different orientation. This altered binding orientation of DABE at the hydrophobic region may be due to the differential binding interactions at the specificity pocket.

The lowest energy-binding mode of ABAP to FXa is shown in Figure 7a. In this predicted complex, the naphthamidine group binds to the hydrophobic box region. As can be seen from the stereo diagram, the naphthamidine ring is favorably stacked over the Trp-215 ring. In addition the amidine hydrogens attached to the napthamidine group favorably interact with the side-chain non-polar atoms of Tyr-99 and Phe-174. The orientation of the naphthamidine group at the hydrophobic box is slightly different from the orientation of the hydrophobic group in the DABE complex. The amidine hydrogen attached to the naphthamidine group forms a hydrogen bond with the main chain carbonyl of the Glu-97 (see Figure 7a). The linker carboxylic acid group of ABAP is placed near the side chain of Gln-192 but not with good hydrogen bonding geometry. In the dockings without an active site water molecule, the binding mode of ABAP to FXa is similar but the linker carboxylic group is placed in good hydrogen bonding position to the side chain of Gln-192 (Fig 7b). In the second lowest energy complex, the ABAP binds in an extended conformation. In this binding mode the naphthamidine group is placed away from the hydrophobic box and no stacking interactions are possible. The linker carboxylic acid group of ABAP forms two hydrogen bonds with the side chain amidine hydrogens of Gln-192 and Arg-143. In these low energy complexes of ABAP the

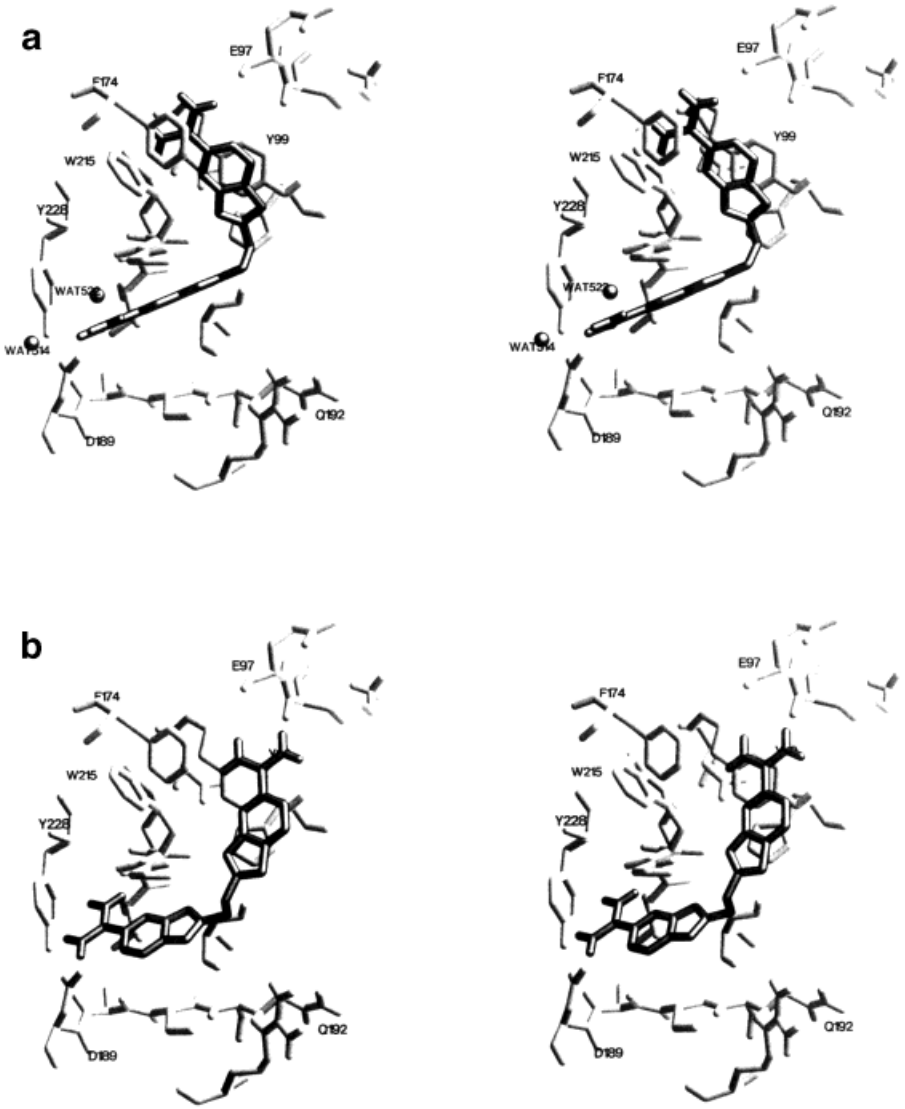

Fig. 7. Mode of binding of ABAP to FXa: **(a)** with solvent and **(b)** without solvent.

amidine group forms three hydrogen bonds with the specificity pocket residues and WAT522.

The top ranking binding mode of DX-9065a to FXa both in the absence and presence of water molecules are shown in Figure 8a and b. It is very clear from these figures that the general mode of binding is the same in both the cases. However, in the presence of water molecules the orientation of the amidine group is confined to the Asp-189 side chain. In the lowest energy complex (Figure 8a), the amidine group attached to the naphthamidine binds into the specificity pocket and forms three hydrogen bonds with the specificity pocket residue Asp-189 and WAT522. The linker carboxylic group favorably interacts with the side chains of Gln-192. The pyrolidine group binds in the hydrophobic region. This binding mode is in agreement with the model proposed by other groups.[19,20] In addition to the above interactions in our model, a hydrogen bond is possible between the amidine hydrogen attached to the pyrolidine group of DX-9065a and the main chain carbonyl of Lys-96 and Glu-97.

After initial preparation of this manuscript the X-ray structure of the FXa-DX-9065a complex at 3.0 Å was reported.[28] The binding geometry of this X-ray structural complex was characterized by two sets of interactions—namely the napthamidine group at the specificity pocket and the pyrolidine group at the hydrophobic box region—similar to our predicted complex. Interestingly, the crystal structure reveals a closing-in of the binding pocket by a movement of the Gln-192 side chain. Since the current AutoDock procedure assumes rigid protein geometry, no such movement could be predicted. However as can be seen in Figure 9, both the X-ray structure and our predicted docking show similar interaction between Gln-192 and the linker carboxyl group of DX-9065a. The maintenance of the hydrogen bonding interactions at this site and

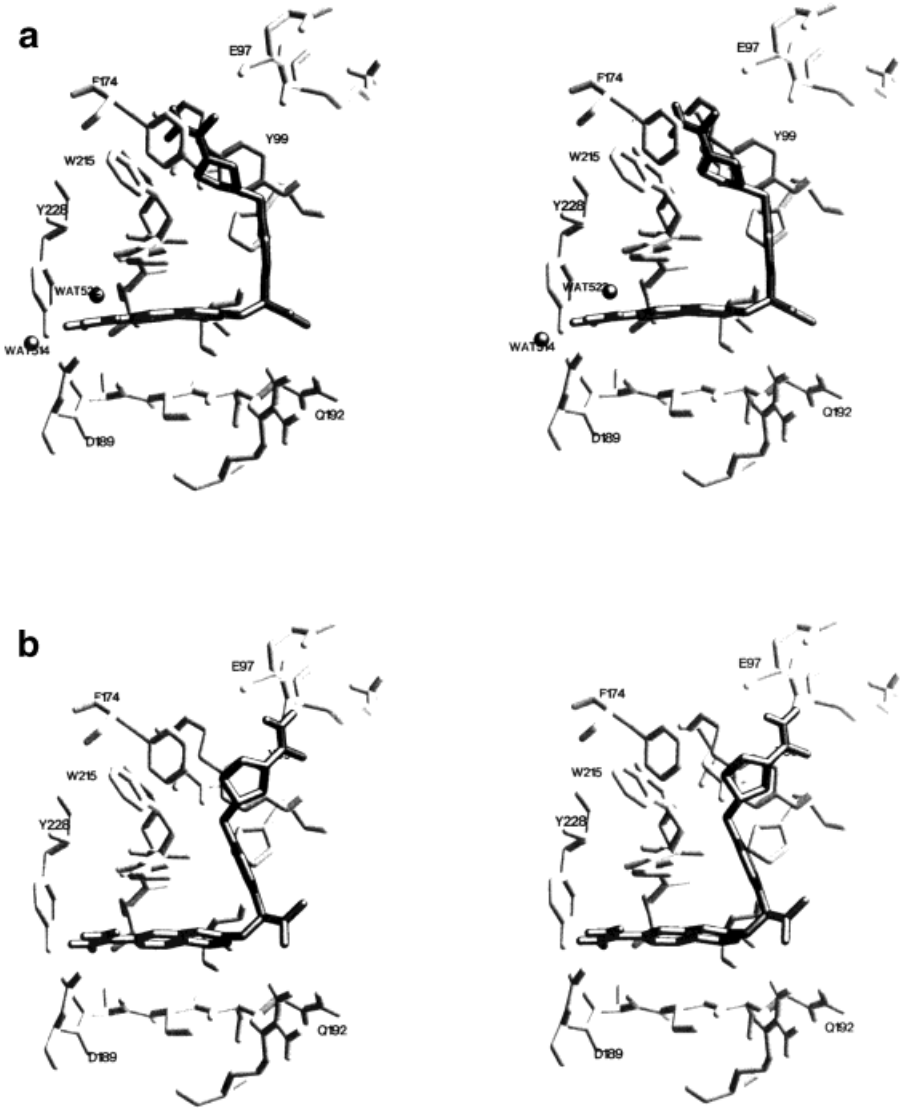

Fig. 8. Modes of binding of DX-9065a to FXa: **(a)** with solvent and **(b)** without solvent.

at the specificity pocket within the larger binding site assumed in the computational docking has produced a substrate conformation that fills the cavity, changing the details of the interaction at the hydrophobic box. The overall RMSD between this lowest-energy model of DX-9065a and that of the X-ray structure is 2.25 Å.

Figure 10 shows the top 5 clustered binding modes of the DX-9065a complex predicted both with and without explicit solvent. All of these predicted binding complexes show interactions at the specificity pocket. For both solvent models, three out of five of the top clusters show hydrophobic interactions at the S4 (hydrophobic box) site. In the other low energy clusters, alternate interactions are seen with nearby hydrophobic patches on the Xa surface. Most of these interactions take place at a site comprised of Phe-94, His-57, and the Tyr-99, which is also a component of the S4 site. A site more distal to S4 is formed by Phe-41, Ala-61, and Gln-192 and is contacted by a few docked conformers. For the other large inhibitors (DABE and ABAP) we find a very similar distribution of dockings among the top five clusters with both solvent models. It is possible that these alternate sites may play a role in macromolecular substrate binding to FXa.

CONCLUSIONS

These docking studies have provided following insights into the possible binding modes of inhibitors to FXa.

i) The amidine group on each of the synthetic inhibitors is involved in hydrogen bonding with the specificity pocket residue Asp-189 of FXa. In all the predicted complexes, the amidine group of the bound inhibitor forms a hydrogen bond with the conserved active site water molecule (WAT522).

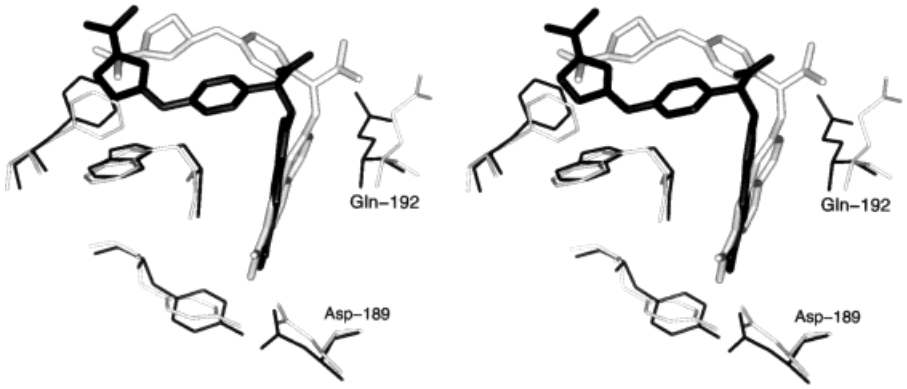

Fig. 9. Stereo diagram showing the superposition of the lowest-energy computed model of DX-9065a with the X-ray structure, in the context of relevant FXa amino acid residues. Thick black and white structures correspond to the experimental and computed inhibitors, respectively. The thin black and white structures correspond to the amino acid positions of the complexed X-ray structure and the uncomplexed FXa X-ray structure used in the docking, respectively.

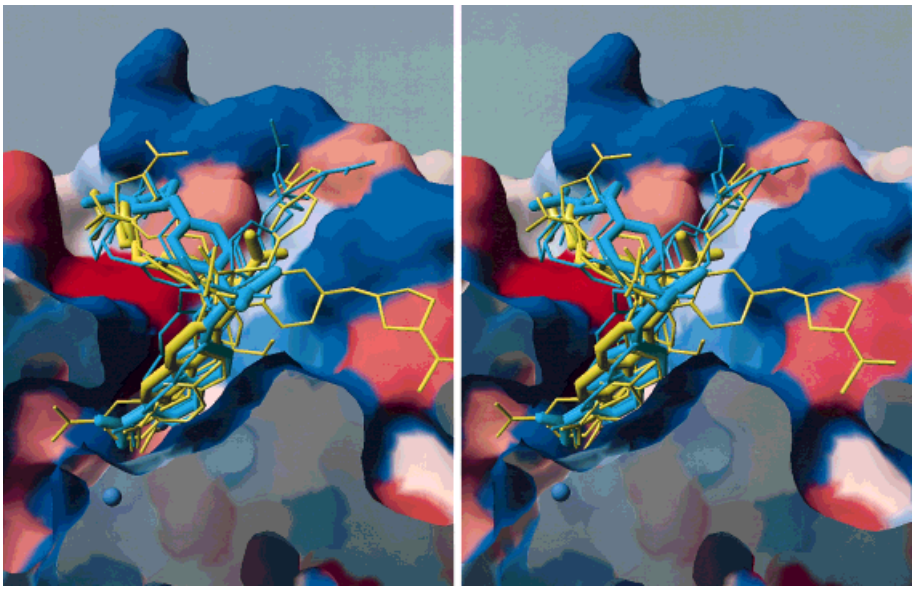

Fig. 10. Stereo diagram showing superposition of low energy conformers of DX-9605a, from the top 5 clusters, on the surface of FXa color-coded by a hydrophobicity scale. Red to blue corresponds to hydrophobic to hydrophilic character. The more saturated the color the stronger the property. The blue stick molecules are those predicted in the presence of active site waters and the yellow colored stick models are those computed in absence of active site water molecules. The thick blue and yellow structures are the computed lowest energy complexes of DX-9605a in the presence and absence of solvent, respectively.

ii) In the predicted complexes of DABE, DX-9065a, and ABAP, the hydrophobic ring portion of the inhibitors favor similar interactions with the hydrophobic box residues Phe-174, Tyr-99, and Trp-215 of FXa. These favorable interactions explain the increased binding affinity of these inhibitors over ABP and APPA.

iii) In the lowest energy complexes of DX9065a and ABAP, the side chain of Gln-192 interacts with the bound inhibitor. These favorable interactions explain the importance of Gln at this location. Recall that Gln192Glu mutation reduces the inhibitory activity by 30-fold of the Kunitz-type inhibitors. In DABE, ABP, and APPA complexes of FXa there is no interaction involving the side chain of Gln-192. These results suggest that Gln-192 plays an important role in discriminating high from low affinity inhibitors.

iv) The addition of a functional group in the 3- or 4- position of the benzamidine ring does not alter the preferred binding interaction of the amidine group with the specificity pocket.

In addition, the docking results using receptor models both with and without active site water molecules correctly discriminate between the higher affinity inhibitors such as DABE, ABAP, and DX-9065a from the lower affinity inhibitors ABP and APPA. The binding energies of the top ranking complexes of higher affinity inhibitors such as ABAP and DX-9065a and lower affinity inhibitors

3ABP agree with experimentally observed binding energies. For these complexes, the predicted binding energies for the top ranking binding modes are within 2 kcal/mol of the experimental values when desolvation and entropic terms are included. The predicted energies for 4ABP, 3APPA, and DABE are lower than the experimental energies. Although the dockings using the model without active site water molecules correctly predicted the general mode of binding and binding energies, they predicted interactions of the ligands with the active site Tyr-228, which may not be possible in the presence of a conserved water molecule (WAT522). Low energy computed binding modes showing alternate hydrophobic interactions may be relevant to macromolecular substrate interactions with Xa.

ACKNOWLEDGMENTS

We thank David Goodsell and Michael Johnson for helpful comments and critical reading of the manuscript. This is publication number 10299-MB of the Scripps Research Institute.

REFERENCES

1. Furie B, Furie B. The molecular basis of coagulation. Cell 1988;53:505–518.
2. Hertzberg M. Biochemistry of Factor X. Blood Rev 1994;8:56–62.
3. Bronz GJ. Tissue factor pathway inhibitor and the current concept of blood coagulation. Blood Coagul Fibrolysis 1995;6:s7–s13.
4. Davie EW, Fujikawa K, Kisiel W. The coagulation cascade: Interaction, maintenance and regulation. Biochemistry 1990;30: 10363–10370.
5. Stubbs MT, Bode W. Coagulation factors and their inhibitors Curr Opin Struct Biol 1994;4:823–832.
6. Hauptmann J, Markwardt F, Walsmann P. Synthetic inhibitors of serine proteinases: Influence of 3 and 4 amidino benzyl derivatives on the formation and action of thrombin. Thromb Res 1978;12:735–744.
7. Tidwell RR, Webster WP, Shaver SR, Geratz JD. Strategies for anticoagulation with synthetic protease inhibitors: Xa inhibitors verses thrombin inhibitors. Thromb Res 1980;19:339–349.
8. Nagahara T, Yokoyama Y, Inamura K, Katakura S, Komoriya S, Yamaguchi H, Hara T, Iwamoto M. J Med Chem 1994;37:1200–1207.
9. Yamaguchi H, Yamada K, Kanetani N, Yokayama Y., inventors. Dibanic (amidinoanyl) propanic acid derivatives as novel blood coagulation Factor Xa inhibitors. Patent 05078344,893 Japan; 1993.
10. Waxman L, Smith DE, Arcuri KE, Vlasuk GP. Tick Anticoagulant Peptide (TAP) is a novel inhibitor of blood coagulation factor Xa. Science 1990;248:593–596.
11. Vlasuk GP. Structural and functional characterization of Tick Anticoagulant Peptide: A potent and selective inhibitor of blood coagulation factor Xa. Thromb Haemost 1994;70:212–216.
12. Padmanaban K, Padmanaban KP, Tulinsky A et al. Structure of human des (1–45) factor Xa at 2.2 Å resolution. J Mol Biol 232:947–966,1993.
13. Smalas AO, Hordvik A. Structure determination and refinement of benzamidine-inhibited trypsin from the north atlantic salmon. Acta Crystallogr Sect D 1993;49:318–330.
14. Tulinsky A. Molecular interactions of thrombin. Semin Thromb Hemost 1996;22:117–124.
15. Rezaie AR, Esmon CT. Contribution of residue 192 in factor Xa to enzyme specificity and function. J Biol Chem 1995;270:16176–16181.
16. Sturzebecher J, Markwardt F, Walsmann P. Synthetic inhibitors of proteinasaes: Inhibiton of Factor Xa by derivatives of benzamidine. Thromb Res 1976;9:637–646.
17. Ishihara H, Hara T, Yokoyama A, Nagahara T, Iwamoto M. Prolongation of coagulation time due to the inhibition of factor Xa by DX-9065a, an orally active synthetic anticoagulant specific for factor Xa. Thromb Haemost 1993;69:671.
18. Katakura S, Nagahara T, Hara T, Iwamoto M. A novel factor Xa inhibitor: Structure-activity relationships and selectivity between factor Xa and thrombin. Biochem Biophys Res Commun 1993;197: 965–972.
19. Lin Z, Johnson ME. Proposed cation-pi mediated binding by factor Xa: A novel enzymatic mechanism for molecular recognition. FEBS Lett 1995;370:1–5.
20. Stubbs MT, Huber R, Bode W. Crystal structures of factor Xa specific inhibitors in complex with trypsin: Structural grounds for inhibition of factor Xa and selectivity against thrombin. FEBS Lett 1995;375:103–107.
21. Goodsell DS, Olson AJ. Automated docking of substrates to proteins by simulated annealing. Proteins 1990;8:195–202.
22. Morris GM, Goodsell DS, Huey R, Olson AJ. Distributed automatic docking of flexible ligands to proteins: Parallel applications of AutoDock 2.4. J Comput Aided Mol Des 1996;10:293–304.
23. Goodford PJ. A computational procedure for determining energetically favorable binding sites on biologically important macromolecules. J Med Chem 1985;28:849–857.
24. Stouten PFW, Frommel C, Nakamura H, Sander C. An effective solvation term based on atomic occupancies for use in protein simulations. Mol Simulations 1993;10: 97–120.
25. Bohm H-J. The development of a simple empirical scoring function to estimate the binding constant for a protein-ligand complex of known three-dimensional structure. J Comput Aided Mol Des 1994;8:243–256.
26. Morris GM, Goodsell DS, Halliday RS et al. Automated docking using a Lamarckian genetic algorithm and an empirical binding free energy function. J Comput Chem 1998;19:1639–1662.
27. Rao MS, Olson AJ. Modes of binding of synthetic inhibitors to FXa, IUCr, Seattle, USA. Conference Proceedings. PS03.05.11:C-90, 1996.
28. Brandstetter H, Kuhne A, Bode W et al. X-ray structure of active site-inhibited clotting factor Xa. Implications for drug design and substrate recognition. J Biol Chem 1996;271:29988–29992.